AD-A105 864 NAVAL POSTGRADUATE SCHOOL MONTEREY CA F/G 20/8
CERENKOV RADIATION PRODUCED BY 100 MEV ELECTRONS.(U)
JUN 81 D E MCLAUGHLIN

UNCLASSIFIED NL

END
DATE
FILMED
DTIC

LEVEL II

(2)

AD A105864

NAVAL POSTGRADUATE SCHOOL
Monterey, California

THESIS

CERENKOV RADIATION PRODUCED BY
100 MeV ELECTRONS

by

David Earl McLaughlin

June 1981

Thesis Advisor: Fred R. Buskirk

Approved for public release; distribution unlimited

UNCLASSIFIED
SECURITY CLASSIFICATION OF THIS PAGE (When Data Entered)

REPORT DOCUMENTATION PAGE

READ INSTRUCTIONS BEFORE COMPLETING FORM

1. REPORT NUMBER

2. GOVT ACCESSION NO. AD-A105 864

3. RECIPIENT'S CATALOG NUMBER (9)

4. TITLE (and Subtitle)
Cerenkov Radiation Produced by 100 MeV Electrons.

5. TYPE OF REPORT & PERIOD COVERED
Master's Thesis; June 1981

6. PERFORMING ORG. REPORT NUMBER

7. AUTHOR(s)
David Earl McLaughlin

8. CONTRACT OR GRANT NUMBER(s)

9. PERFORMING ORGANIZATION NAME AND ADDRESS
Naval Postgraduate School
Monterey, California 93940

10. PROGRAM ELEMENT, PROJECT, TASK AREA & WORK UNIT NUMBERS

11. CONTROLLING OFFICE NAME AND ADDRESS
Naval Postgraduate School
Monterey, California 93940

12. REPORT DATE
June 1981

13. NUMBER OF PAGES
48 pages

14. MONITORING AGENCY NAME & ADDRESS (if different from Controlling Office)
12, 41

15. SECURITY CLASS. (of this report)
Unclassified

15a. DECLASSIFICATION/DOWNGRADING SCHEDULE

16. DISTRIBUTION STATEMENT (of this Report)
Approved for public release; distribution unlimited

17. DISTRIBUTION STATEMENT (of the abstract entered in Block 20, if different from Report)

18. SUPPLEMENTARY NOTES

19. KEY WORDS (Continue on reverse side if necessary and identify by block number)
Stimulated Cerenkov radiation, superluminal, LINAC beam monitor.

20. ABSTRACT (Continue on reverse side if necessary and identify by block number)

It is proposed that electromagnetic radiation of a specified frequency can be produced as a result of stimulated Cerenkov radiation in a dielectric resonator excited by a superluminal electron beam. The frequency generated is a function of three physical parameters. They are the electron energy, the thickness of the dielectric resonator and its index of refraction. This work provides a theoretical derivation for predicting the frequency

Item 20 (contd)

of stimulated Cerenkov radiation in a dielectric slab. The first experimental results using extremely relativistic electrons are reported, and the problems encountered are outlined with some suggestions for improvements. The results of this validation show that the observed frequency differs from the predicted frequency by less than 1.5%. Incidental to the conduct of this experiment, ordinary Cerenkov radiation in the usual cone was observed in air at microwave frequencies. A possible application of the stimulated Cerenkov process as an electron beam monitor is briefly discussed.

Appoved for public release; distribution unlimited

Cerenkov Radiation Produced by 100 MeV Electrons

by

David Earl McLaughlin
Lieutenant Commander, United States Navy
B.S.M.E., Michigan State University, 1969

Submitted in partial fulfillment of the
requirements for the degree of

MASTER OF SCIENCE IN PHYSICS

from the

NAVAL POSTGRADUATE SCHOOL
June 1981

Author: David E. McLaughlin

Approved by: Fred R Buskirk
Thesis Advisor

J N Dyer
Second Reader

J N Dyer
Chairman, Department of Chemistry and Physics

William M. Tolles
Dean of Science and Engineering

ABSTRACT

It is proposed that electromagnetic radiation of a specified frequency can be produced as a result of stimulated Cerenkov radiation in a dielectric resonator excited by a superluminal electron beam. The frequency generated is a function of three physical parameters. They are the electron energy, the thickness of the dielectric resonator and its index of refraction. This work provides a theoretical derivation for predicting the frequency of stimulated Cerenkov radiation in a dielectric slab. The first experimental results using extremely relativistic electrons are reported, and the problems encountered are outlined with some suggestions for improvements. The results of this validation show that the observed frequency differs from the predicted frequency by less than 1.5%. Incidental to the conduct of this experiment, ordinary Cerenkov radiation in the usual cone was observed in air at microwave frequencies. A possible application of the stimulated Cerenkov process as an electron beam monitor is briefly discussed.

TABLE OF CONTENTS

LIST OF TABLES

LIST OF FIGURES

ACKNOWLEDGEMENTS

The author wishes to express his gratitude to his thesis advisor, Professor Fred R. Buskirk, for his instruction, guidance and assistance in all phases of this project.

Thanks are also extended to Professor J. Knorr of the Naval Postgraduate School's Electrical Engineering Department for providing equipment and for his many helpful suggestions in the course of this work, and to Professor John E. Walsh of Dartmouth College for his encouragement.

The assistance of Mr. Don Snyder in the fabrication of the experimental setup and in the day-to-day operation and maintenance of the NPS LINAC is greatly appreciated.

Finally, the author wishes to thank his wife, Catherine, for her understanding, patience and support throughout this work and for her assistance in composition and proofreading.

I. INTRODUCTION

Cerenkov radiation, the radiation which is generated by a charged particle moving at superluminal velocity in a medium has been considered as a possible radiation source for many years. Additionally, Cerenkov radiation has been used as a charged particle detector which will selectively detect only charged particles exceeding the speed of light in the medium through which they are traveling. This detection is dependent upon only the velocity of the particle and the index of refraction of the medium. The detector is a simple photocell and as such does not distinguish between frequencies within its band of operability. Recently, Professor John E. Walsh [Ref. 1] reported successful generation of Cerenkov radiation using relativistic electrons and a dielectric resonator in the form of a cylindrical anulus. The import of Walsh's work is that the frequency of the radiation generated in the dielectric is a function only of the energy of the electrons, the thickness of the dielectric, and the index of refraction of the dielectric. Since these quantities are material parameters, it would appear that radiation of any desired frequency could be obtained by selecting the proper set of parameters.

The intent of this experiment is to extend Walsh's work, using a different geometry for the dielectric resonator and

much higher electron energies. Professor Walsh conducted his experiments at 300 KeV in contrast to the present experiment, which uses electron energies in the 10-100 MeV range, an increase of 1.5 to 2 orders of magnitude. In this experiment, radiation in the X band was selected for ease of measurement and analysis, with a view to extending the work into the IR range.

II. THEORY

Consider a dielectric slab with a coordinate system as shown in Figure 1. The dielectric has thickness h in the z direction and is unbounded in the x and y directions. There is a dielectric-conductor interface at z=0 which lies in the x-y plane. The dielectric slab has permittivity ε and permeability μ_0 while these quantities are ε_0 and μ_0, respectively, in vacuum.

Starting with Maxwell's equations and following the usual procedure, it can be shown that the longitudinal components, E_x or H_x, satisfy a wave equation and the modes can be divided into TE or TM modes. The general expressions for the transverse components of the wave equation solution are:

$$H_y = \frac{i\omega\varepsilon}{\omega^2\mu\varepsilon-k^2}\frac{\partial E_x}{\partial z} - \frac{ik}{\omega^2\mu\varepsilon-k^2}\frac{\partial H_x}{\partial y} \tag{1}$$

$$F_z = \frac{-ik}{\omega^2\mu\varepsilon-k^2}\frac{\partial E_x}{\partial z} + \frac{i\omega\mu}{\omega^2\mu\varepsilon-k^2}\frac{\partial H_x}{\partial y} \tag{2}$$

$$E_y = \frac{-i\omega\mu}{\omega^2\mu\varepsilon-k^2}\frac{\partial H_x}{\partial z} - \frac{ik}{\omega^2\mu\varepsilon-k^2}\frac{\partial E_x}{\partial y} \tag{3}$$

$$H_z = \frac{-ik}{\omega^2\mu\varepsilon-k^2}\frac{\partial H_x}{\partial z} - \frac{i\omega\varepsilon}{\omega^2\mu\varepsilon-k^2}\frac{\partial E_x}{\partial y} \tag{4}$$

The intent of this experiment is to take energy from a beam of electrons in the vacuum just above the dielectric slab

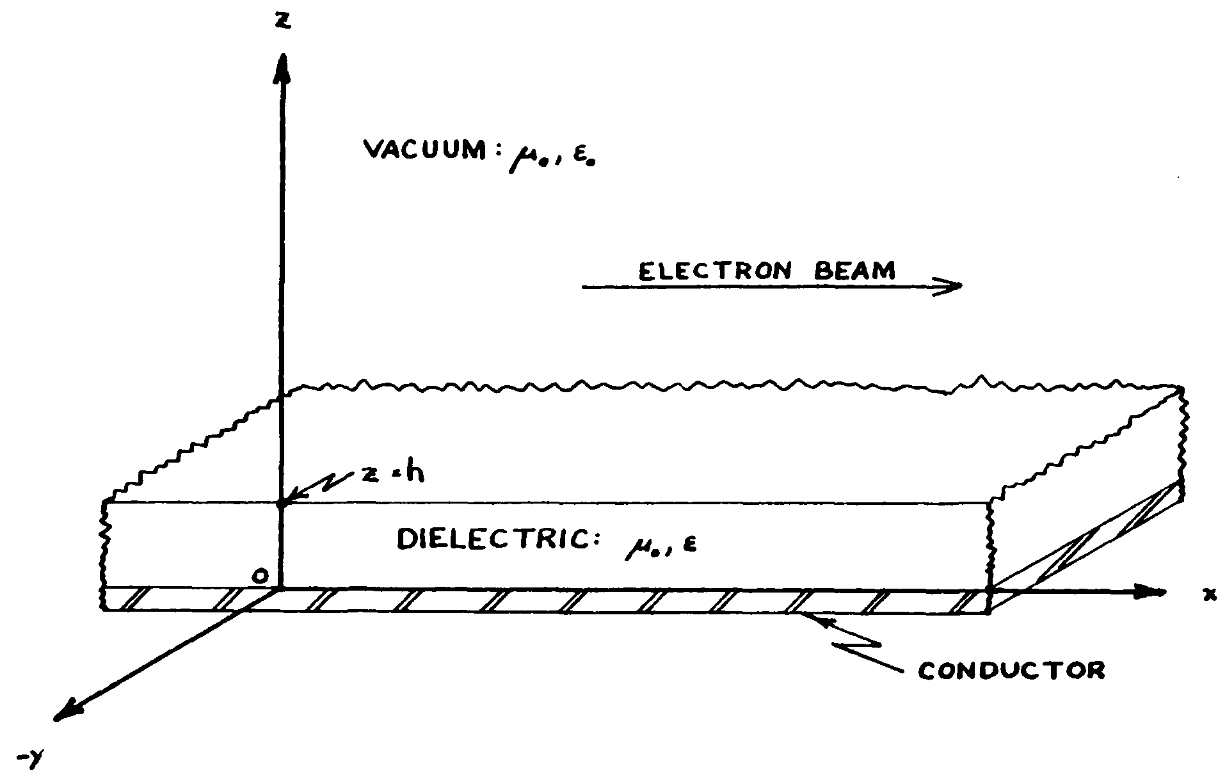

COORDINATE SYSTEM

FIGURE 1.

and give this energy to an EM wave in the slab and in the vacuum above the slab. This energy transfer requires a component of $\vec{E}$ in the x-direction. Therefore, the wave in the dielectric should be TM mode. Thus, for TM modes where $H_x=0$ and E_x exist, the wave equation for E_x is:

$$(\nabla_\perp^2 + \{\omega^2\mu\varepsilon - k^2\})E_x = 0 \tag{5}$$

When the condition that $H_x=0$ is applied to Equations 1, 2, 3 and 4, the result is

$$H_y = \frac{i\omega\varepsilon}{\omega^2\mu\varepsilon-k^2}\frac{\partial E_x}{\partial z} \tag{6}$$

$$E_z = \frac{-ik}{\omega^2\mu\varepsilon-k^2}\frac{\partial E_x}{\partial z} \tag{7}$$

$$E_y = \frac{-ik}{\omega^2\mu\varepsilon-k^2}\frac{\partial E_x}{\partial y} \tag{8}$$

$$H_z = \frac{-i\omega\varepsilon}{\omega^2\mu\varepsilon-k^2}\frac{\partial E_x}{\partial y} \tag{9}$$

For simplicity, let

$$\omega^2\mu_0\varepsilon_0 - k^2 = -a^2 \tag{10}$$

for waves propagating in vacuum and let

$$\omega^2\mu_0\varepsilon - k^2 = b^2 \tag{11}$$

for waves propagating in the dielectric. Assuming no y dependence, which is appropriate for a slab which extends to infinity in the + and - y directions, Eq. 5 reduces to

$$\frac{\partial^2 E_x}{\partial z^2} + (\omega^2\mu\varepsilon - k^2)E_x = 0 \tag{12}$$

Thus, in vacuum, substituting Eq. 10 into Eq. 12 yields

$$\frac{\partial^2 E_x}{\partial z^2} - a^2 E_x = 0 \tag{13}$$

which, when the restriction that E_x goes to zero as z goes infinity is applied, has as its solution

$$E_x = Ae^{-az} \tag{14}$$

Similarly, substituting Eq. 11 into Eq. 12 for the dielectric case yields

$$\frac{\partial^2 E_x}{\partial z^2} + b^2 E_x = 0 \tag{15}$$

When the boundary condition of a conductor at the origin is imposed, the solution to Eq. 15 is

$$E_x = B \sin (bz) \tag{16}$$

At the vacuum-dielectric interface, the usual boundary conditions apply. That is, the tangential components of $\vec{E}$ and $\vec{H}$ must be continuous and the normal components of $\vec{D}$ and $\vec{B}$ must also be continuous. For this problem, with the given coordinate system, the tangential components of $\vec{E}$ are E_x and E_y, the tangential components of $\vec{H}$ are H_x and H_y. The normal component of $\vec{D}=\varepsilon\vec{E}$ is εE_z and the normal component of $\vec{B}=(1/\mu)\vec{H}$ is $\frac{1}{\mu}H_z$. E_y and H_y are zero when the assumption of no y dependence is applied to Eqs. 8 and 9 and for TM modes H_x is zero by definition. Thus, the boundary conditions reduce to: E_x, H_y and εE_z must all be continuous at the

vacuum-dielectric interface. Equating Eqs. 14 and 16 at z=h and applying the boundary condition of continuity to E_x leads to

$$Ae^{-ah} = B \sin (bh) \tag{17}$$

Making the appropriate substitutions into either Eqs. 6 or 7 and applying the continuity requirement for εE_z at z=h results in the same equation.

$$\frac{i\omega\varepsilon_0(-aAe^{-ah})}{-a^2} = \frac{i\omega\varepsilon(bB \cos\{bh\})}{b^2} \tag{18}$$

This reduces to

$$\frac{\varepsilon_0 Ae^{-ah}}{a} = \frac{\varepsilon B \cos(bh)}{b} \tag{19}$$

Equations 17 and 19 comprise a coupled set of equations which must be simultaneously satisfied.

The following development indicates one method of solution which leads to an expression for the propagation constant, k, and the corresponding phase velocity for the propagating mode. Dividing Eq. 17 by Eq. 19 gives

$$\frac{a}{\varepsilon_0} = \frac{b}{\varepsilon} \tan (bh) \tag{20}$$

$$\frac{\varepsilon}{\varepsilon_0} a = b \tan (bh) \tag{21}$$

$$\frac{\varepsilon}{\varepsilon_0} ah = bh \tan (bh) \tag{22}$$

Let y=ah and x=bh

$$y = \frac{\varepsilon_0}{\varepsilon} x \tan x \tag{23}$$

Applying the definition of the index of refraction (n)

$$y = \frac{x \tan x}{n^2} \tag{24}$$

Recalling the definitions of a^2 and b^2 and adding them

$$a^2 + b^2 = \omega^2\mu_0(\varepsilon-\varepsilon_0) \tag{25}$$

$$a^2h^2 + b^2h^2 = \omega^2\mu_0(\varepsilon-\varepsilon_0)h^2 \tag{26}$$

Substituting for $(ah)^2$ and $(bh)^2$

$$y^2 + x^2 = \omega^2\mu_0(\varepsilon-\varepsilon_0)h^2 \tag{27}$$

The right hand side of Eq. 26 is a constant, which we will call R^2

$$y^2 + x^2 = R^2 \tag{28}$$

The simultaneous solution of Eqs. 23 and 28 for a given frequency will result in the value of k which yields fields satisfying all boundary conditions. A representative solution of this system of equations with n=1.461 (polyethylene) is shown in Figure 2.

Although the TM modes are the desired modes, it is necessary to also consider the TE modes to see if there is any degeneracy. Equations 1, 2, 3 and 4 reduce to

$$H_y = \frac{-ik}{\omega^2\mu\varepsilon-k^2}\frac{\partial H_x}{\partial y} \tag{29}$$

$$E_z = \frac{i\omega\mu}{\omega^2\omega\varepsilon-k^2}\frac{\partial H_x}{\partial y} \tag{30}$$

$$E_y = \frac{-i\omega\mu}{\omega^2\mu\varepsilon-k^2}\frac{\partial H_x}{\partial z} \tag{31}$$

$$H_z = \frac{-ik}{\omega^2\mu\varepsilon-k^2}\frac{\partial H_x}{\partial z} \tag{32}$$

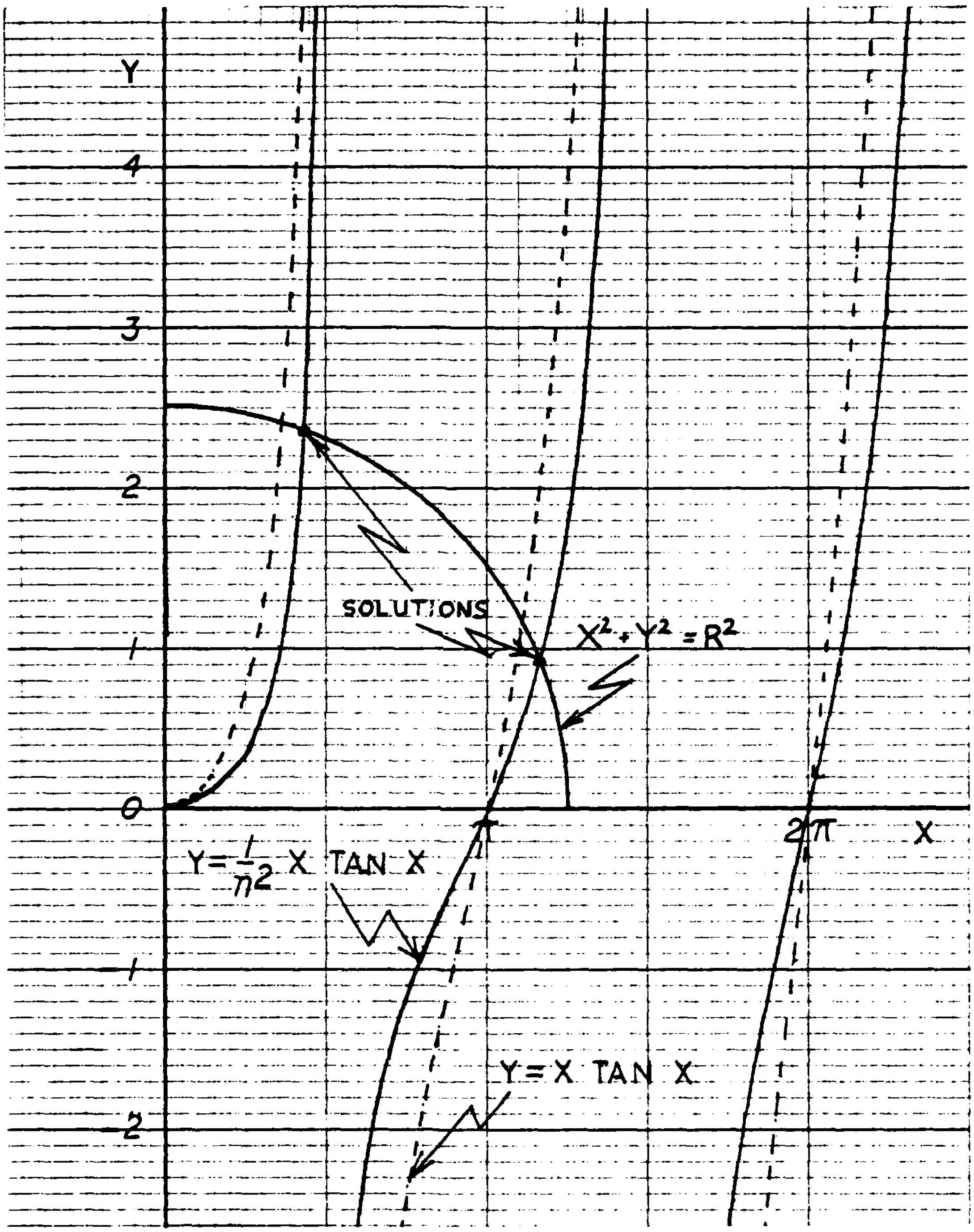

GRAPHICAL SOLUTION

FIGURE 2.

The TE mode wave equation for H_x is

$$(\nabla_\perp^2 + \{\omega^2\mu\varepsilon - k^2\})H_x = 0 \tag{33}$$

Again, assuming no y dependence, Eq. 33 becomes

$$\frac{\partial^2 H_x}{\partial z^2} + (\omega^2\mu\varepsilon - k^2)H_x = 0 \tag{34}$$

Substituting Eq. 10 into Eq. 34 for waves propagating in vacuum

$$\frac{\partial^2 H_x}{\partial z^2} - a^2 H_x = 0 \tag{35}$$

which has a solution

$$H_x = Ce^{-az} \tag{36}$$

and substituting Eq. 11 into Eq. 34 for waves is the dielectric

$$\frac{\partial^2 H_x}{\partial z^2} + b^2 H_x = 0 \tag{37}$$

which has a solution

$$H_x = D \sin (bz) \tag{38}$$

when the appropriate boundary condition at z=0 is imposed.

The same requirements for the vacuum-dielectric interface apply. The assumption of no y dependence immediately makes Eqs. 29 and 30 zero. The remaining tangential component of $\vec{H}$ is H_x, the remaining tangential component of $\vec{E}$ is E_y and for the normal components of $\vec{D}$ and $\vec{B}$, only $B_z = \frac{1}{\mu}H_z$ remains. These three components must be continuous at the interface

at z=h. Thus

$$Ce^{-ah} = D \sin (bh) \tag{39}$$

and

$$\frac{-i\omega\mu_0 \, (-aCe^{-ah})}{-a^2} = \frac{-i\omega\mu_0 \, (bD \cos \{bh\})}{b^2} \tag{40}$$

$$\frac{Ce^{-ah}}{a} = \frac{D \cos (bh)}{b} \tag{41}$$

Dividing Eq. 39 by Eq. 41,

$$a = b \tan (bh) \tag{42}$$

$$ah = bh \tan (bh) \tag{43}$$

Again. letting y=ah and x=bh,

$$y = x \tan x \tag{44}$$

Equations 27 and 28 are still valid and the simultaneous solution of Eqs. 28 and 44 will satisfy all boundary conditions for a given frequency.

The simularity between Eq. 44 and Eq. 23 indicates that both TE and TM modes will propagate at about the same frequency in the dielectric. However, only the TM mode is capable of gaining energy from the electrons. Accordingly, if stimulated Cerenkov radiation is observed, it will be the TM modes that are excited. If, however, an attempt is made to amplify waves fed into the dielectric from some outside source, some mechanism must be found to exclude the TE mode waves from being introduced into the dielectric.

A clearer picture of the relationships can be seen by use of geometry. First, define

$$k_f^2 = \omega^2 \mu_0 \varepsilon_0 \tag{45}$$

the magnitude of the free space k vector for a plane wave and

$$k_d^2 = \omega^2 \mu_0 \varepsilon \tag{46}$$

the magnitude of the k vector for a plane wave in the dielectric. Substituting these into Eqs. 10 and 11, the defining equations for a^2 and b^2 respectively, yields after multiplication by h^2,

$$k_f^2 h^2 - k^2 h^2 = -a^2 h^2 \tag{47}$$

$$k_d^2 h^2 - k^2 h^2 = b^2 h^2 \tag{48}$$

Subtracting Eq. 47 from Eq. 48

$$R^2 = h^2 k_d^2 - h^2 k_f^2 \tag{49}$$

or

$$R^2 + h^2 k_f^2 = h^2 k_d^2 \tag{50}$$

This defines a right triangle as shown in Figure 2. Rearranging the terms in Eq. 47 defines another right triangle,

$$a^2 h^2 + k_f^2 h^2 = k^2 h^2 \tag{51}$$

also shown in Figure 3. Note that the side $k_f h$ is common to both triangles and that the magnitude of the unknown k, the wave number of the propagating mode in the dielectric that satisfies all the boundary conditions, is between k_f and k_d. There is an important consequence of this development.

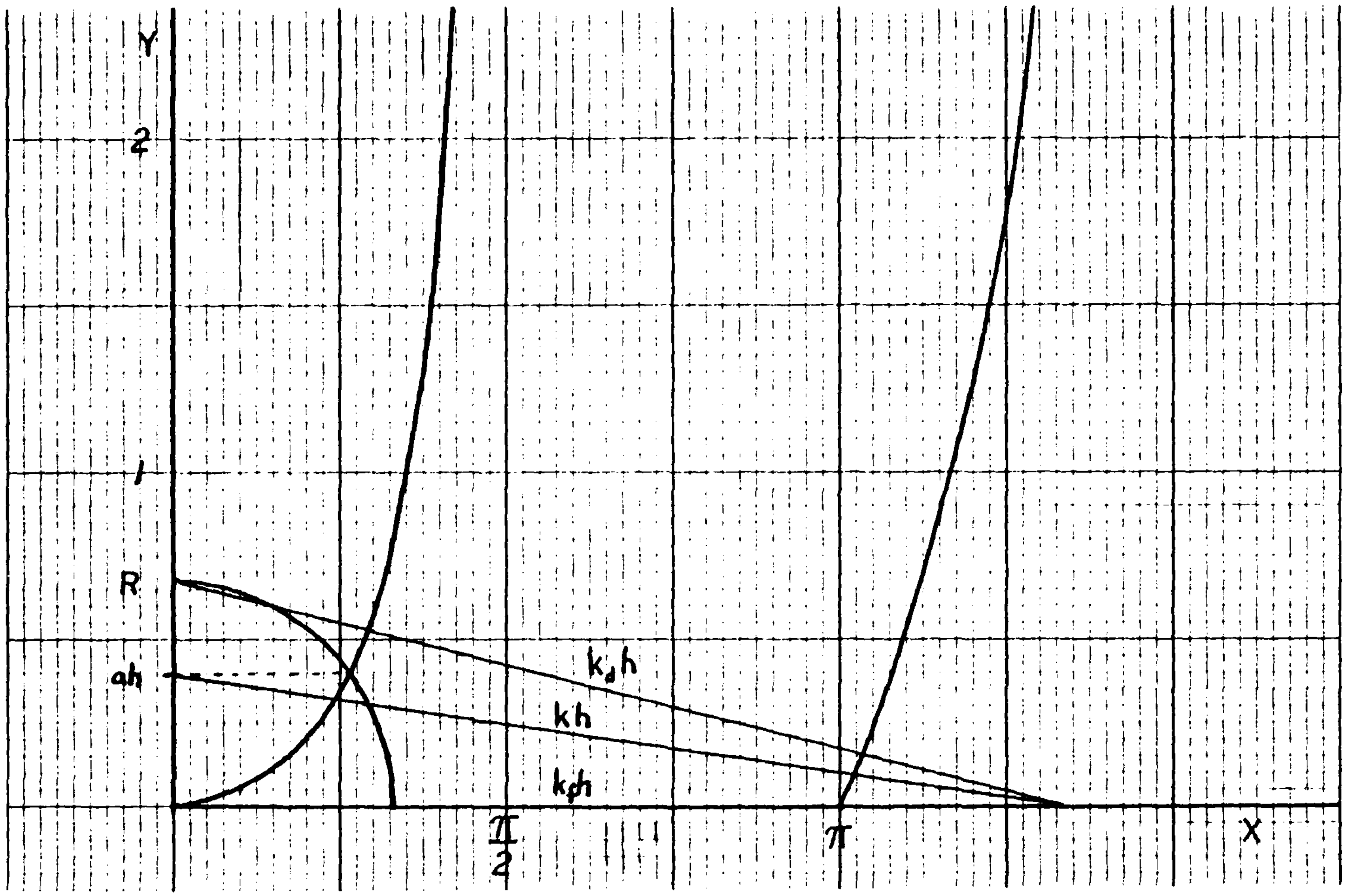

GEOMETRIC RELATIONSHIPS

FIGURE 3.

Since, for energy exchange, the phase velocity of the wave in the dielectric, as represented by the unknown, k, must be matched to the velocity of the electrons. Also the velocity of the electrons must be less than the speed of light in the medium above the dielectric. Thus the region above the dielectric must be in vacuum because 100 MeV electrons have a velocity slightly faster than the velocity of a plane wave in air under normal conditions.

At this point it is possible to proceed to a numerical solution. First, by phase matching the velocity of the electrons to the velocity of the stimulated wave in the dielectric

$$v_{el} = v_{mode} \tag{52}$$

By definition

$$\beta = \frac{v}{c} \tag{53}$$

and after applying Eq. 52

$$\beta c = v_{mode} \tag{54}$$

Again, by definition

$$k_{mode} = \frac{\omega}{v_{mode}} \tag{55}$$

$$k_{mode} = \frac{\omega}{\beta c} \tag{56}$$

and

$$\gamma^2 = \frac{1}{1-\beta^2} \tag{57}$$

$$\beta^2 = \left(1 - \frac{1}{\gamma^2}\right) \tag{58}$$

Substituting Eq. 58 into Eq. 56

$$k_{mode} = \frac{\omega}{(1 - \frac{1}{\gamma^2})^{\frac{1}{2}} c} \qquad (59)$$

Thus, k_{mode} is determined for a given γ and ω. Once ω is specified, Eqs. 45 and 46 specify k_f and k_d. Rearranging Eq. 10 and substituting Eq. 45 yields

$$a^2 = k_{mode}^2 - k_f^2 \qquad (60)$$

$$a = (k_{mode}^2 - k_f^2)^{\frac{1}{2}} \qquad (61)$$

Similarly

$$b^2 = (k_d^2 - k_{mode}^2) \qquad (62)$$

$$b = (k_d^2 - k_{mode}^2)^{\frac{1}{2}} \qquad (63)$$

Solving Eq. 21 for h

$$\frac{\varepsilon a}{\varepsilon_0} = b \tan (bh) \qquad (21)$$

$$\frac{\varepsilon a}{\varepsilon_0 b} = \tan (bh) \qquad (64)$$

$$bh = \tan^{-1} (n^2 \frac{a}{b}) \qquad (65)$$

$$h = \frac{1}{b} \tan^{-1} (n^2 \frac{a}{b}) \qquad (66)$$

Thus, given a desired frequency, ω, the index of refraction of the dielectric, n, and the energy of the electrons, γ, the thickness of the dielectric can be determined.

The substitution of Eq. 59 into Eqs. 10 and 11 allows the factoring out of ω^2 and Eq. 66 becomes

$$h = \frac{1}{\omega\left(\mu_0\varepsilon - \frac{1}{(1-\frac{1}{\gamma^2})c^2}\right)^{\frac{1}{2}}} \tan^{-1}\left\{n^2 \frac{\left(\frac{1}{(1-\frac{1}{\gamma^2})c^2} - \mu_0\varepsilon\right)^{\frac{1}{2}}}{\left(\mu_0\varepsilon - \frac{1}{(1-\frac{1}{\gamma^2})c^2}\right)^{\frac{1}{2}}}\right\} \quad (67)$$

which can be solved for ω given h, n, and γ.

$$\omega = \frac{1}{h\left(\mu_0\varepsilon - \frac{1}{(1-\frac{1}{\gamma^2})c^2}\right)^{\frac{1}{2}}} \tan^{-1}\left\{n^2 \frac{\left(\frac{1}{(1-\frac{1}{\gamma^2})c^2} - \mu_0\varepsilon\right)^{\frac{1}{2}}}{\left(\mu_0\varepsilon - \frac{1}{(1-\frac{1}{\gamma^2})c^2}\right)^{\frac{1}{2}}}\right\} \quad (68)$$

The significance of Eq. 68 is that the physical parameters of h, n, and γ specify ω. With the proper selection of these parameters, EM radiation of any frequency can be generated.

Examination of Figure 2 readily shows that if the dimensionless parameter bh exceeds π, more than one solution is possible. However, these modes will be at different frequencies and the graphical solution indicates that, if $x<3\pi$, the single desired frequency can be extracted by use of a band-pass or high pass filter.

III. EXPERIMENTAL EQUIPMENT AND PROCEDURE

It was decided to conduct this experiment in the X-band (8-12 GHz) after consulting with Professor Knorr and investigating the availability of the necessary equipment and measuring devices needed to support the experiment. The dielectric chosen was polyethelyne which has an index of refraction of 1.461 [Ref. 2]. The Naval Postgraduate School's Linear Accelerator (LINAC) is capable of producing relativistic electrons with energies up to 120 MeV. The operating characteristics of the NPS LINAC can be found in Appendix A.

A TI-59 programmable calculator program was developed to solve Eqs. 67 and 68. An explanation of this program and a listing of it can be found in Appendix B. Table I shows the input parameter values and the program's solution of Eq. 66 for the 0, 1 and 2 modes.

TABLE I

THICKNESSES OF POLYETHELYNE FOR MODES 0,1,2

m	E [MeV]	n	f [FHz]	h[mm] [1]
0	50	1.461	10	.095
1	50	1.461	10	14.07
2	50	1.461	10	28.15

[1] Program output value

Based on these results, a thickness of 12.7mm (0.5 in) was selected. The values of E=50 MeV, n=1.461, h=12.7mm for a Mode 1 solution predict a frequency of 11.08 GHz when the TI-59 program solves Eq. 68.

The beam of the LINAC is approximately 1 cm in diameter. The width of the dielectric was made to be 5.08 cm to approximate the infinite slab in the y direction. The end of the dielectric away from the LINAC exit window was tapered to fit into an X-band hollow waveguide and to facilitate the TM to TE transition required since a TE mode is the lowest mode that will propagate in a hallow waveguide. Figure 4 is a photograph of the dielectric resonator as it was originally configured.

The first attempt to observe the desired EM radiation met with only limited success. The dielectric slab was mounted about 1 cm below the centerline axis of the LINAC exit window in air. The metal waveguide was sloped slightly to allow clear passage of the electrons over the top of the flange connector to the detector. A diode detector was used with its output lead to an oscilliscope (CRO). With a beam energy of 53.85 MeV and an average beam current[2] of 8.0 nAmp, the CRO display showed a pulse of about 1 μsec with strength varying from 100-200 mV as the beam was tuned, focused and

[2]All currents read on a secondary emission monitor with 6% efficiency, and the monitor current is reported in this work.

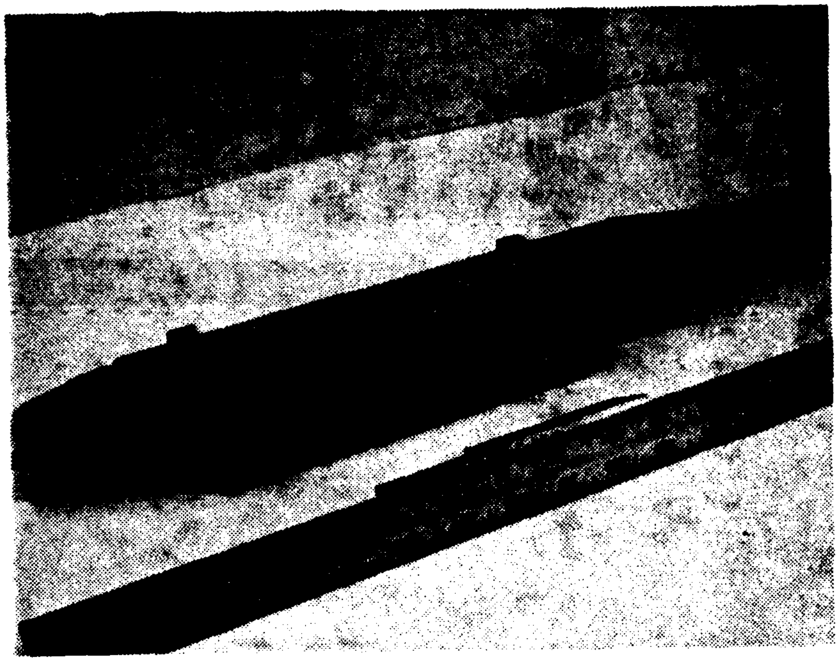

DIELECTRIC RESONATOR

FIGURE 4.

varied in distance from the slab. However, attempts to measure the frequency with a high Q calibrated cavity resonator were unsuccessful.

To determine if the observed pulse was caused by the dielectric, the slab was removed leaving the hollow waveguide in place. When the beam was turned on, a 0.5 microsecond pulse of slightly reduced magnitude was observed. At this point, it was realized that the observed pulse might be caused by Cerenkov radiation in air. Although commonly accepted as 1.0, the actual index of refraction of standard dry air is 1.003 [Ref. 3]. Using this value as β^{-1} it can be easily shown that electrons with energies exceeding 20.856 MeV will exceed the speed of light in standard dry air. Thus, electrons above that energy would exceed the velocity of a plane wave in air, and could not be matched to the TM mode velocity.[3]

A simple experiment was designed to investigate this possibility. The equipment arrangement is shown in Figure 5. The reflector used was a thin sheet of aluminum which would allow the passage of the electrons and reflect any EM radiation. With the reflector in place, a pulse was observed from detector 2 whose magnitude was approximately 0.5 times the magnitude of the output from detector 1. When the reflector was removed, a pulse of magnitude 0.1 times the output of

[3]See Section II.

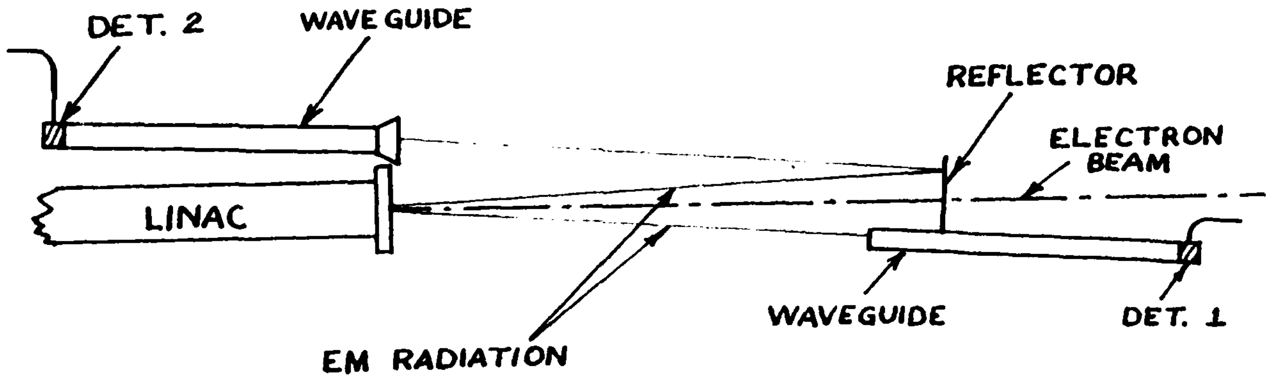

AIR CERENKOV EXPERIMENTAL SETUP

FIGURE 5.

detector 1 was observed from detector 2. These results support the hypothesis of air Cerenkov. Since the air Cerenkov should be very broadband, no attempt was made at this time to measure the frequency of this radiation.

Based on these results, it was decided to enclose the dielectric slab in a vacuum chamber. Figure 6 is a photograph of the interior of the vacuum chamber. The vacuum was maintained in the chamber by installing a 1/16 in. thick piece of polyethelyne between two waveguide flanges exterior to the chamber. A waveguide run of about 75 ft. was added to the setup which allowed for the positioning of the detector in the LINAC control room thus eliminating the long, lossy coaxial cable runs. A Tektronic 491 Spectrum Analyzer (491-S/A) [illegible] obtained to facilitate frequency analysis.

The use [illegible] this new setup with team energy of 100.97 MeV, beam current of 4.3 nA and the same diode detector used before resulted in a 0.5 Volt peak pulse of about 1 microsecond duration. The increase in peak output was attributed to the reduction in line loss provided by the replacement of the coax cable by waveguide. Subsequent tests, which will be discussed later, have modified this hypothesis. The 491-S/A, with a 20 dB attenuator inserted between the waveguide to coax adapter and the S/A, detected signals at 12.39 GHz and 8.57 GHz. The 12.39 GHz signal was the image of a real signal above the frequency range of the 491-S/A. Using a relatively low Q cavity, it was determined that most of the

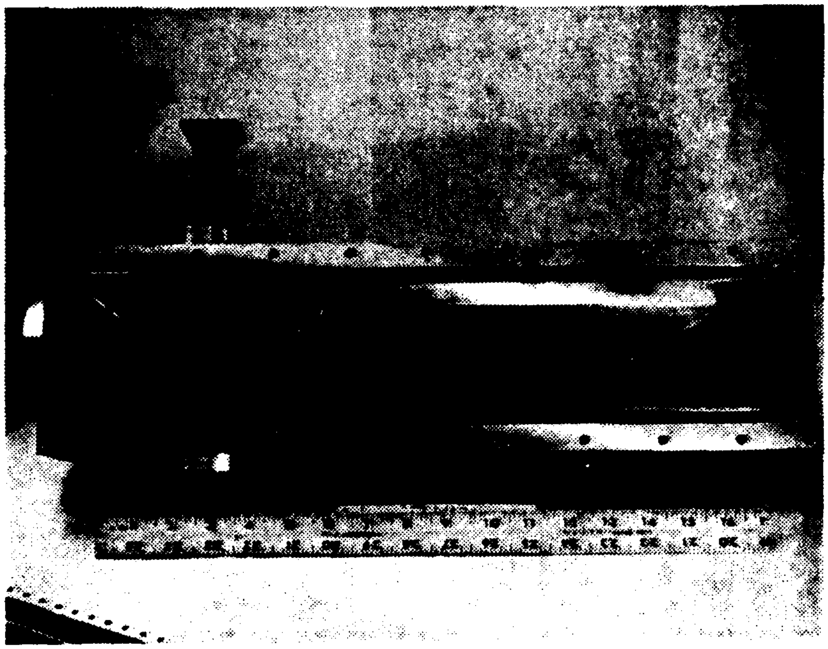

VACUUM CHAMBER

FIGURE 6.

power in the pulse was in the 8.57 GHz signal. A dispersive high pass filter with a cutoff frequency of 9.9 GHz was installed between the waveguide from the dielectric and the coax adapter. With this arrangement and no attenuation at the input of the 491-S/A, valid signals were detected at 8.58, 8.99 and 11.42 GHz. When the dielectric was removed from the vacuum chamber and the test repeated, the same signals were detected. Both with and without dielectric, all signals disappeared when electron injection was interrupted with LINAC RF power maintained.

The 8.57 GHz and 11.48 GHz signals appear to be the third and fourth harmonics of the LINAC operating frequency. The exact cause of the 8.99 GHz signal is not known but it is believed to be caused by a resonant mode of the vacuum chamber. The chamber is a rectangular aluminum box with 10 mil aluminum windows for electron entry and exit and as such would act as a cavity resonator. Equipment limitations prevent the measurement of any change in strength of the 11.48 GHz signal with and without the dielectric slab in place. This frequency is only 4% above the predicted frequency for the given parameters and it is possible that the desired signal is hidden by the LINAC harmonic at that frequency. Also, the actual index of refraction of the polyethylene was not experimentally determined and it was not manufactured specifically for optical use. It is possible that a slight change in n and/or inhomogeneities in the material could cause some frequency shifting.

Additional tests were conducted with this configuration. Two anomalies were observed which required further explanation. First, an intermittent, valid signal was detected at 10.24 GHz. This signal is not fully understood but it is believed to be extraneous to the experiment. Secondly, the peak output of the diode detector varied as much as an order of magnitude with the same beam parameters and beam position.

This observation led to a more intensive investigation of the TM to TE coupling at the dielectric/waveguide transition. In particular, for the m=1 mode, it was realized that cancellation of the E-field could occur at the transition point. A graphical representation of the E-field in the dielectric is shown in Figure 7. It was decided to nullify the lower field at the transition by inserting a vertical conductor into the dielectric slab at the mouth of the waveguide as shown in Figure 8. The vertical conductor should not affect any TE modes propagating in the dielectric but should nullify the cancellation effect of the m=1 mode for any TM mode waves propagating in the dielectric. Another modification of the setup was also made at this time. The 10 mil. aluminum window between the LINAC and the vacuum chamber was replaced by a 10 mil. mylar window to minimize beam spreading at the entrance to the vacuum chamber.

Table II shows the results of the frequency analysis of the dielectric with and without the conductor in place. The beam parameters were as follows: E=65.29 MeV, I=4.0 nA.

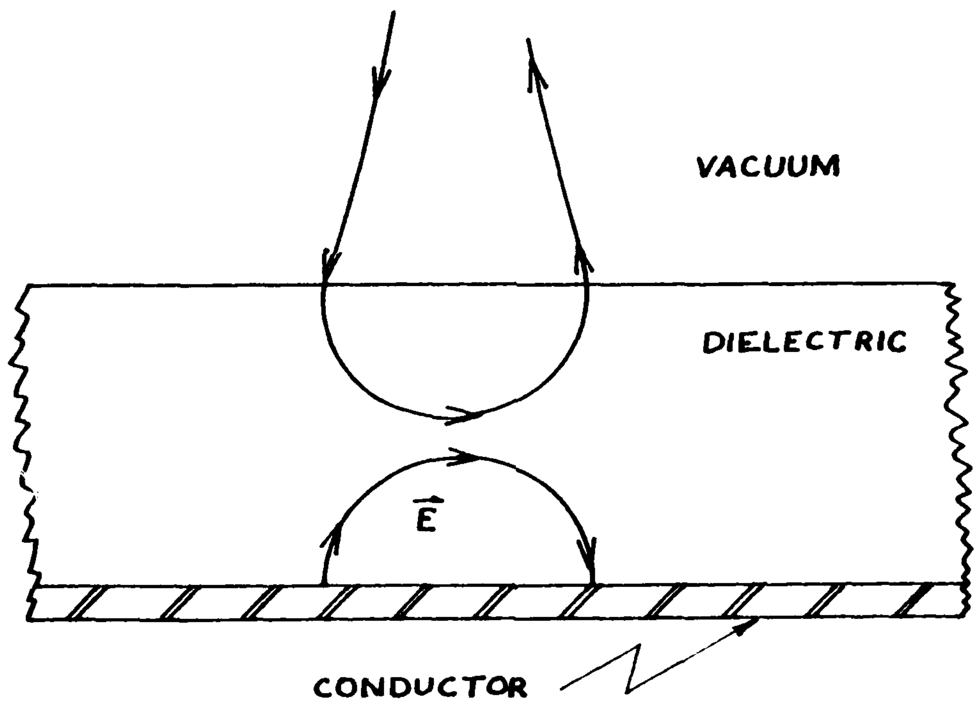

E-FIELD IN THE DIELECTRIC

FIGURE 7.

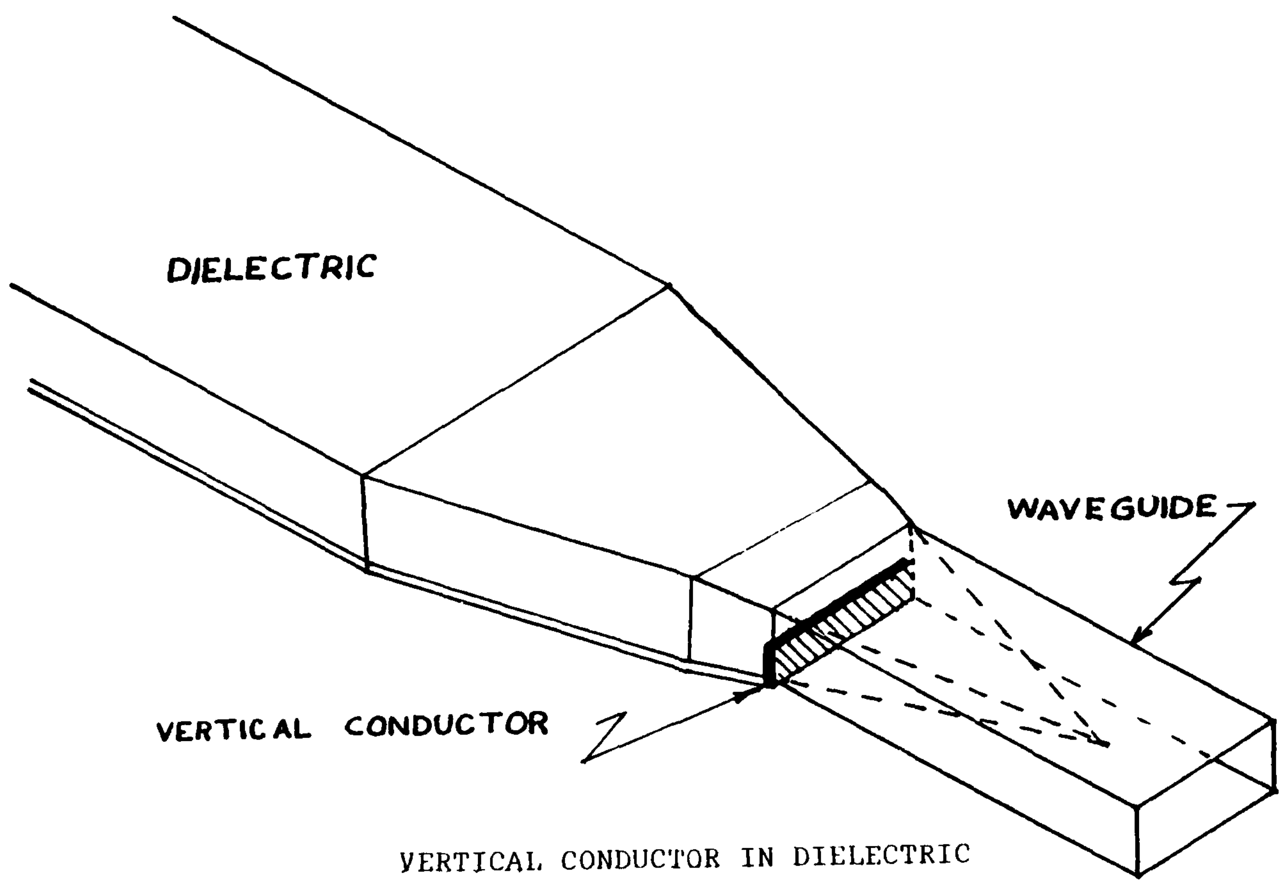

VERTICAL CONDUCTOR IN DIELECTRIC

FIGURE 8.

TABLE II

FREQUENCIES OBSERVED

With Conductor		Without Conductor	
f [GHz]	Strength	f [GHz]	Strength
8.57	very strong	8.57	strong
9.00	moderate	9.00	weak
9.52	weak	----	----
10.21	moderate	10.25	moderate
10.92	weak	----	----
11.42	strong	11.50	moderate

The peak voltage observed from the diode detector was 150 mV without the vertical conductor and 100 mV with the conductor in place. It is interesting to note that although half of the area of the waveguide was blocked, the detector voltage dropped by only about one third.

For input values of E=65.29 MeV, n=1.461, h=12.7 mm and m=1, the TI-59 program predicts a frequency of 11.08 GHz. The 9.52 GHz signal does not correspond to any predicted frequency. Possible explanations of this frequency will be discussed later. The observed 10.92 GHz signal is only 1.4% below the predicted value. Since this frequency is only observed when the vertical conductor is in place, it is believed that this is a TM mode resulting from stimulated Cerenkov radiation.

IV. DISCUSSION AND CONCLUSIONS

It appears from the foregoing experiment that stimulated Cerenkov radiation can be produced at the predicted frequency with the proper choice of parameters. The 1.4% error can be explained in several ways. First, the predicted frequency is based on an algorithm that provides an approximate solution for modes where $m>0$. Second, nonoptical quality polyethylene was used for the dielectric slab. Finally, the theoretical development assumed an infinite slab in the y direction. In fact, a finite slab was used whose y dimension was about 5 times the diameter of the focused beam. Any one of the deviations from the ideal case or a combination of them could account for the error. The most probable source of error is the index of refraction of the polyethylene. An index of refraction of 1.473, a change of 0.012 which is less than 1% of the tabulated value in Ref. 3, would reduce the error to essentially zero.

The cause of the TM mode frequency at 9.52 GHz shown in Table II is not fully understood. It could be a result of the edge effects caused by the finite width of the dielectric or it might be a resonant TM mode of the vacuum chamber.

A secondary effect observed during the course of this experiment is worth noting. When the focused beam was passed above the dielectric, the output of the diode detector

varied with the beam current. This effect was present both in air and in vacuum. It may be possible to construct a calibration curve of diode voltage vs. beam current and thereby develop a beam current measuring device which does not destroy the beam downstream from the measurement point as the beam current measuring device presently in use does.

It is readily apparent from the magnitude of the diode pulse that the stimulated Cerenkov radiation effect is very inefficient. To match the mode with high speed electrons requires that the component of the mode's E-field parallel to the electron beam be small compared with the field's transverse components. This will tend to make the coupling small. The output power of the diode detector is less than 0.5 mWatts. Most of this power, conservatively estimated at 95%, is in the 8.57 GHz signal as demonstrated in Section III. This does, however, enhance the possibility of developing an electron beam current meter, based on this process, which has only a minimal effect on the beam itself.

The results of this experiment support the hypothesis that stimulated Cerenkov radiation can be produced at a frequency specified by the physical parameters of electron energy, index of refraction and dielectric thickness. It appears that the wave-electron coupling is a weak effect which is further degraded by the TM to TE coupling used to extract the signal in this experiment. Greater efficiency may be possible if a more effective means of extracting the

signal is developed. The signal itself may be increased in strength by lengthening the dielectric slab to increase the length of the wave-electron interaction region.

Additional work in the area of stimulated Cerenkov radiation appears to be warranted. The development presented here is not guaranteed to be unique. There may be other modes that can be stimulated in the dielectric, one of which might provide a stronger signal. A mode with a larger longitudinal component could increase the electron-mode coupling. Additionally, the effect of the pulsed beam of electrons should be studied in depth. Specifically, the question of why this experimental setup produces most of its output power at the third harmonic of the LINAC operating frequency should be investigated in greater detail. If the power in the LINAC harmonics can be shifted to the Cerenkov frequency it would greatly increase the usefulness of the stimulated Cerenkov process as a radiation source. Finally, generation of X-band radiation using the m=0 mode should be attempted as a preliminary step in extending this work into the IR range. The dielectric thickness predicted by the theoretical development presented here for an IR generator is of the order of microns. The X-band m=0 thickness is in this range. Extracting a signal from a dielectric this thin may cause some difficulties. The experience thus gained should be valuable in extending this work into the IR range.

APPENDIX A

LINAC OPERATING CHARACTERISTICS

Max Energy	120 MeV
Max Average Current	3-5 microAmp
Operating Frequency	2.856 GHz
PRF	60 pps
Pulse Duration	1.0 microseconds
Nr. of Klystrons	3
Peak Output Power per Klystron	21 MWatts

APPENDIX B

TI-59 PROGRAM LISTING AND EXPLANATION

This program does not use any library programs within the algorithm. The inputs are the electron beam energy (in MeV), the index of refraction of the dielectric (dimensionless), either the desired frequency (in Hz) or the dielectric thickness (in meters), and the mode (dimensionless). The mode input determines which leg of the $y=(1/n^2)x \tan x$ in the curve (in the first quadrant) is used. For a given m=0,1,2... the solution is found for x values such that $m\pi<x<[(2m+1)\pi/2]$. As noted in Chapter II, if $x>\pi$, more than one solution is possible. This program solves only for the solution in the $m\pi<x< [(2m+1)\pi/2]$ range.

The solution for m=0 is unique and exact. Solutions for higher order modes are found using an iterative search. The solution is approximate in that the program searches down the designated leg of $y=(1/n^2)x \tan x$ in discrete steps until it finds a y value less than the y value for the corresponding m=0 case. This value of y is then taken as the solution point for the input mode.

To solve Equation 67:

1. Load program.
2. Enter E[MeV], press A.

3. Enter n, press B.

4. Enter f[nz], press C.

5. Enter m, press E.

The program will solve for h [meters].

To solve Equation 68:

1. Load program.

2. Enter E[MeV], press A.

3. Enter n, press B.

4. Enter h[m], press D.

5. Enter m, press E'.

The program will solve for f[Hz].

The program listing is on the following pages.

000	76	LBL
001	11	A
002	57	ENG
003	55	÷
004	93	.
005	05	5
006	01	1
007	01	1
008	95	=
009	42	STO
010	00	00
011	91	R/S
012	76	LBL
013	12	B
014	33	x^2
015	42	STO
016	01	01
017	65	X
018	08	8
019	93	.
020	08	8
021	05	5
022	04	4
023	01	1
024	01	1
025	08	8
026	52	EE
027	94	+/-
028	01	1
029	02	2
030	42	STO
031	02	02
032	95	=
033	42	STO
034	03	03
035	04	4
036	52	EE
037	94	+/-
038	07	7
039	65	X
040	89	π
041	95	=
042	42	STO
043	04	04
044	91	R/S
045	76	LBL
046	13	C
047	65	X
048	02	2
049	65	X
050	89	π
051	95	=
052	42	STO
053	05	05
054	91	R/S
055	76	LBL
056	14	D
057	42	STO
058	06	06
059	91	R/S
060	76	LBL
061	15	E
062	42	STO
063	07	07
064	67	EQ
065	19	D'
066	71	SBR
067	88	DMS
068	71	SBR
069	68	NOP
070	43	RCL
071	13	13
072	65	X
073	43	RCL
074	11	11
075	95	=
076	42	STO
077	14	14
078	71	SBR
079	58	FIX
080	42	RCL
081	15	15
082	33	x^2
083	85	+
084	43	RCL
085	17	17
086	33	x^2
087	95	=
088	55	÷
089	53	(
090	43	RCL
091	10	10
092	75	-
093	43	RCL
094	09	09
095	54	)
096	95	=
097	34	$\sqrt{x}$
098	42	STO
099	18	18
100	91	R/S
101	76	LBL
102	18	C7
103	01	1
104	42	STO
105	05	05
106	71	SBR
107	88	DMS
108	71	SER
109	69	OP
110	55	÷
111	02	2
112	55	÷
113	89	π
114	95	=
115	91	R/S
116	76	LBL
117	19	D'
118	71	SBR
119	88	DMS
120	71	SBR
121	68	NOP
122	91	R/S
123	76	LBL
124	10	E'
125	42	STO
126	07	07
127	67	EQ
128	18	C'
129	01	1
130	42	STO
131	05	05
132	71	SBR
133	88	DMS
134	71	SBR
135	69	OP
136	43	RCL
137	08	08
138	75	-
139	43	RCL
140	09	09
141	95	=
142	34	$\sqrt{x}$
143	65	X
144	43	RCL
145	19	19
146	65	X

147	43	RCL
148	06	06
149	95	=
150	42	STO
151	14	14
152	71	SBR
153	58	FIX
154	43	RCL
155	15	15
156	33	x^2
157	85	+
158	43	RCL
159	17	17
160	33	x^2
161	95	=
162	55	÷
163	43	RCL
164	06	06
165	33	x^2
166	55	÷
167	53	(
168	43	RCL
169	10	10
170	75	-
171	43	RCL
172	09	09
173	54	)
174	95	=
175	34	$\sqrt{x}$
176	42	STO
177	20	20
178	55	÷
179	02	2
180	55	÷
181	89	π
182	95	=
183	91	R/S
184	76	LBL
185	88	DMS
186	43	RCL
187	00	00
188	33	x^2
189	35	1/x
190	94	+/-
191	85	+
192	01	1
193	95	=
194	65	X
195	02	2
196	93	.
197	09	9
198	09	9
199	07	7
200	09	9
201	02	2
202	05	5
203	52	EE
204	08	8
205	33	x^2
206	95	=
207	35	1/x
208	65	X
209	43	RCL
210	05	05
211	33	x^2
212	95	=
213	42	STO
214	08	08
215	43	RCL
216	05	05
217	33	x^2
218	65	X
219	43	RCL
220	02	02
221	65	X
222	43	RCL
223	04	04
224	95	=
225	42	STO
226	09	09
227	43	RCL
228	05	05
229	33	x^2
230	65	X
231	43	RCL
232	03	03
233	65	X
234	43	RCL
235	04	04
236	95	=
237	42	STO
238	10	10
239	43	RCL
240	08	08
241	75	-
242	43	RCL
243	09	09
244	95	=
245	34	$\sqrt{x}$
246	42	STO
247	11	11
248	43	RCL
249	10	10
250	75	-
251	43	RCL
252	08	08
253	95	=
254	34	$\sqrt{x}$
255	42	STO
256	12	12
257	92	RTN
258	76	LBL
259	68	NOP
260	43	RCL
261	01	01
262	65	X
263	43	RCL
264	11	11
265	55	÷
266	43	RCL
267	12	12
268	95	=
269	70	RAD
270	22	INV
271	30	TAN
272	55	÷
273	43	RCL
274	12	12
275	95	=
276	42	STO
277	13	13
278	92	RTN
279	76	LBL
280	69	OP
281	43	RCL
282	01	01
283	65	X
284	43	RCL
285	11	11
286	55	÷
287	43	RCL
288	12	12
289	95	=
290	70	RAD
291	22	INV
292	30	TAN
293	55	÷

294	53	(
295	43	RCL
296	12	12
297	65	X
298	43	RCL
299	06	06
300	54	)
301	95	=
302	42	STO
303	19	19
304	92	RTN
205	76	LBL
306	58	FIX
207	09	9
308	94	+/-
309	22	INV
310	28	LOG
311	85	+
312	43	RCL
313	07	07
314	65	X
315	89	π
316	95	=
317	42	STO
318	15	15
319	01	1
320	01	1
321	94	+/-
322	22	INV
232	28	LOG
324	94	+/-
325	42	STO
326	16	16
327	76	LBL
328	50	|x|
329	43	RCL
330	15	15
331	70	RAD
332	30	TAN
333	65	X
334	43	RCL
335	15	15
336	55	÷
337	43	RCL
338	01	01
339	95	=
340	42	STO
341	17	17
342	75	-
343	43	RCL
344	14	14
345	95	=
346	22	INV
347	77	GE
348	59	INT
349	43	RCL
350	16	16
351	44	SUM
352	15	15
353	61	GTO
354	50	|x|
355	76	LBL
356	59	INT
357	92	RTN

LIST OF REFERENCES

1. Walsh, J. E., "Stimulated Cerenkov Radiation," Physics of Quantum Electronics, Vol. 5, Ed. S. F. Jacobs et al, Addison Wesley Publishing Company, Inc., 1978.

2. Simonis, G. J., "Near mm Wave Materials," Harry Diamond Labs.

3. Hodgman, C. D., Handbook of Chemistry and Physics, 38th Edition, Chemical Rubber Publishing Co., 1956.

INITIAL DISTRIBUTION LIST

		No. Copies
1.	Defense Technical Information Center Cameron Station Alexandria, Virginia 22314	2
2.	Library, Code 0142 Naval Postgraduate School Monterey, California 93940	2
3.	Physics Library, Code 61 Department of Physics and Chemistry Naval Postgraduate School Monterey, California 93940	1
4.	Professor F. R. Buskirk, Code 61Bs Department of Physics and Chemistry Naval Postgraduate School Monterey, California 93940	5
5.	LCDR David E. McLaughlin, USN 1062 Clearspring Lane Virginia Beach, Virginia 23464	1

DAT

FILM